X-ray excited optical luminescence detection by scanning near-field optical microscope: A new tool for nanoscience

Silvia Larcheri and Francesco Rocca[a)]
CNR-IFN, Istituto di Fotonica e Nanotecnologie, Unità "FBK-CeFSA" di Trento, Via alla Cascata 56/C, 38100 Trento, Italy

Frank Jandard and Daniel Pailharey
CRMC-N and Université de la Méditerranée, Campus de Luminy, 13009 Marseille, France

Roberto Graziola
Dipartimento di Fisica, Università di Trento, Via Sommarive 14, 38100 Trento, Italy

Alexei Kuzmin and Juris Purans
Institute of Solid State Physics, University of Latvia, Kengaraga 8, Riga LV-1063, Latvia

(Received 11 October 2007; accepted 26 November 2007; published online 4 January 2008)

Investigations of complex nanostructured materials used in modern technologies require special experimental techniques able to provide information on the structure and electronic properties of materials with a spatial resolution down to the nanometer scale. We tried to address these needs through the combination of x-ray absorption spectroscopy (XAS) using synchrotron radiation microbeams with scanning near-field optical microscopy (SNOM) detection of the x-ray excited optical luminescence (XEOL) signal. This new instrumentation offers the possibility to carry out a selective structural analysis of the sample surface with the subwavelength spatial resolution determined by the SNOM probe aperture. In addition, the apex of the optical fiber plays the role of a topographic probe, and chemical and topographic mappings can be simultaneously recorded. Our working XAS-SNOM prototype is based on a quartz tuning-fork head mounted on a high stability nanopositioning system; a coated optical fiber tip, operating as a probe in shear-force mode; a detection system coupled with the microscope head control system; and a dedicated software/hardware setup for synchronization of the XEOL signal detection with the synchrotron beamline acquisition system. We illustrate the possibility to obtain an element-specific contrast and to perform nano-XAS experiments by detecting the Zn K and W L_3 absorption edges in luminescent ZnO and mixed $ZnWO_4$–ZnO nanostructured thin films. © *2008 American Institute of Physics.*
[DOI: 10.1063/1.2827485]

I. INTRODUCTION

The physics, chemistry, and biology of phenomena occurring in nanoscale systems are a very new subject with its own set of physical principles and theoretical descriptions. These new phenomena strongly need techniques that directly probe the nanosystems at the length scale where they really occur.

Bringing together the broad range of processing tools, characterization equipment, and technical expertise required to span the length scales of interest to nanoscience is a significant challenge. A possible way to address this issue is to use a multimodal approach based on the coupling of different techniques capable of providing chemical as well as structural information.

For instance, the extremely high lateral resolution of scanning probe microscopies (SPMs) makes these techniques leading actors in all domains of nanoscience and nanotechnology. SPMs provide key information on surface morphology and allow a local characterization of a wide number of physical properties, with a resolution going down to the atomic scale.[1,2] Moreover, specific scanning probes allow manipulating and modifying the matter at the nanoscale. Unfortunately, these tools suffer of lack in chemical sensitivity.

On the other hand, x-ray absorption spectroscopy (XAS) probes the average chemical and structural properties around selected atoms, being able to determine chemical composition and state, bond lengths, coordination numbers, and dynamical properties on the atomic scale. However, these are average values. The main limitation of XAS is the lack of spatial resolution, the lateral being coincident with the dimensions of the x-ray beam and the in depth being strongly dependent on the x-ray energy. Currently, big efforts are made aiming to reduce the beam spot size down to the 10–100 nm range, but the possibility of "touching" and mechanically interacting with samples at the nanoscale is a feature that synchrotron radiation itself does not exhibit, despite its importance as characterization tool in the nanoworld.

Thus, SPM and XAS provide complementary information, and it appears extremely tempting to merge them in order to get a deeper insight in physical and chemical properties of materials at the nanoscale.

[a)]Electronic mail: rocca@science.unitn.it.

In this paper we present an instrument based on this idea: it uses the optical fiber tip of a scanning near-field optical microscope (SNOM) to detect the x-ray excited optical luminescence (XEOL) of a sample irradiated with a synchrotron radiation beam. The XAS-SNOM head microscope can be seen as the natural extension of a microprobe instrument having chemical sensitivity and morphology recognition. The main advantage of this approach is that the lateral resolution is determined by the SNOM tip and not by the x-ray spot size.

Two different investigation techniques have been explored within the project:

(1) *element-specific profilometry*, a conventional scanning technique enriched by the sensitivity to distribution of chemical elements, achieved by tuning the x-ray energy below and above the absorption edges of specific elements;
(2) *single-point nano-XAS*, by keeping the local probe at a fixed position on the sample while the x-ray energy is tuned across the absorption edge of an atomic species. As a result, it is possible to obtain the x-ray absorption spectrum relative to a specific chemical element located in the nanoregion probed by the tip.

Beside the improvement of the lateral resolution, one of the most promises of SNOM technique is the development of nondestructive chemical imaging. Up to now, a wide variety of optical properties has been used to generate contrast in near-field imaging, but a technique providing a robust chemical identification still remains elusive.

Raman scattering is currently used by a number of research groups but its small cross section results in very long integration time.[3–5] The imaging of the intensity of infrared absorption from a particular atomic bond (whose cross section is significantly greater than for Raman scattering) has been also recognized as an important new direction for near-field optics[6] (in fact, experimental work in the far infrared was reported already in 1985).[7] A free electron laser (FEL) has also been used with success as a light source to collect infrared transmission spectra with a near-field microscope, but the spatial resolution achieved in these experiments is difficult to be assessed quantitatively.[8,9] More recently, Michaels *et al.*[10] developed an illumination mode IR-SNOM based on a tunable broadband infrared light source and an infrared focal plane array-based spectrometer, which allows parallel detection of the entire pulse bandwidth (200 cm^{-1}). They estimate a spatial resolution of $\lambda/7.5$ at 3.4 μm and an instrumental sensitivity to fractional transmission changes of 1×10^{-3}. A similar apparatus, but operating in collection mode, was employed by Cricenti and co-workers to study boron nitride films and biological specimens.[11–13] Beside obtaining chemical specificity, they present images with resolution of the order of $\lambda/60$ with a SNOM working with infrared light. In all these experiments, the spatial resolution is achieved thanks to near-field detection by optical tips. The alternative apertureless approach used by Knoll and Keilmann[14] and Lahrech *et al.*[15] is notable because of the extremely high spatial resolution that was reported ($\lambda/20$).

Other approaches exist in literature to develop techniques that couple the ability of luminescence mapping and spectroscopic analysis on a microscopic scale with the elemental sensitivity given by x-ray absorption spectroscopy. One has been proposed by Martinez-Criado *et al.* who used a hard, high-brilliant x-ray microbeam to probe the x-ray excited optical luminescence emitted by the sample.[16,17] In that case, the monochromatic beam was focused on the sample to a spot of 0.6×0.9 μm^2 size with a focus depth of 0.4 mm by means of Au Fresnel zone plates as focusing lenses. Various optical contrast images or micro-XEOL spectroscopy at a fixed point on the sample surface were obtained with the spatial resolution offered by the microfocused x-ray beam. A similar technique has been implemented by Hamilton and co-workers to develop luminescence imaging and spectroscopy for optical detection of x-ray absorption spectroscopy (ODXAS).[18,19] In both cases, the lateral resolution is determined by the dimension of the beam (that, in principle, can be reduced to less than 100 nm by using, for example, Fresnel zone plates[20] or refractive lenses[21] or capillary optics[22,23]) and by the scattering of x-ray photons on the surface. However, the topographic characterization of the same area is normally impossible, or is a very hard task. In our configuration, the optical resolution of the XEOL image is determined only by the aperture of the SNOM tip, and the focusing is mainly used to increase the photon density on the investigated region.

The development of a XAS-SNOM local probe microscope to collect XEOL in near-field conditions could represent a step ahead in the construction of tools to investigate matter at the nanoscale but, at the same time, is a real technical and scientific challenge. The problems faced since the beginning of the project touched different realms of science and instrumentation technology. It is worth going through the most important of them.

A. Signal intensity

Leaving aside for a moment the technical problems involved in detection of specific optical photons under x-ray excitation, feasibility is the issue that should be addressed first. In the proposed operational mode, the signal originates from a nanoregion of the sample surface and is picked up by a nanodetector, namely, the SNOM probe. So the question comes down to this: is the signal strong enough to be detected? Thanks to the continuous progresses in x-ray optics, the number of x-ray photons that can be focused down in a synchrotron radiation microbeam is getting more and more high (for instance, 10^{12} photon/s are focused on the sample at the ESRF-ID03 beamline), thus rising the level of signal detectability. Of course, only the implementation of *in situ* experiments using a fully working microscope prototype could confirm or deny the actual feasibility of such a combined technique.

B. The optical probe

Ultrasensitive photon and force detection electronic systems have to be designed and developed in order to record these extremely low signals. The tip itself has to be the object of careful analysis and fabrication. In fact, beside deter-

mining the lateral resolution, the probe, that collects and guides the signal to the detector, represents the active element of the detection system. The tip has to pick up only the signal locally emitted under the probe apex, preventing the collection of other photons, coming from regions different from the investigated one. Thus, it is fundamental to screen the tip's lateral surface with an opaque coating. Another important issue to deal with is the prevention of direct x-ray illumination of the tip. The very intense synchrotron radiation beam could irreversibly damage the tip and its performances. Complete shielding cannot be reached but, in any case, the amount of photons that directly impinge on the tip should be minimized by a careful setup and alignment.

C. Integration at the synchrotron radiation beamline

The XAS-SNOM instrumentation has to be adapted to work in the demanding environment of a synchrotron radiation facility. It has to be compact and easily installable inside the hutch, suiting different experimental and space needs. The XAS-SNOM head scanner as well as the electronic circuitry has to be protected from direct x-ray illumination and from electromagnetic interferences. Custom-tailored software and hardware systems have to be implemented in order to remotely control the instrumentation locked in the experimental hutch and to carry out the signal detection in synchronization with the beamline acquisition system. Another problem to face is the vibration immunity and compensation. Any geometrical fluctuation of the tip with respect to the sample and to the x-ray beam can, in principle, translate in noise and introduce signal modulations, degrading the quality of the measurement. Thus, the instrument should be equipped with an efficient damping system. On the other hand, the synchrotron radiation beam should be as stable as possible at the level of not having large fluctuations with respect to the tip. Finally, a major issue is the implementation of an alignment procedure to correctly place the optical fiber probe with respect to the x-ray microbeam at the submicrometer scale and to keep it at the same position during the measurement.

II. PROTOTYPE INSTRUMENTATION

A. Device design: General choices

Since the near-field detection of the XEOL signal using a SNOM tip is an unprecedented experimental goal, the XAS-SNOM instrumentation has been conceived and developed taking into account the specific constraints and needs of this novel application. According to this:

(1) Attention has been focused on the aperture SNOM configuration, in which an optical fiber tip with a subwavelength aperture at its very apex is used as optical probe. The nature itself of the experiment imposed to operate the instrument in collection mode: the optical fiber tip acts as detector of the x-ray excited optical luminescence emitted by the sample, guiding the photons to the spectrometer or directly to the detector for the spectral/imaging analysis;
(2) The mechanism employed for the tip-sample distance regulation and for the recording of the topographic image is the shear-force tip feedback,[24] which employs a quartz tuning fork vibrating parallel to the sample surface at one of its resonance frequencies. This arrangement leads to a completely open architecture, offering enough space for the incident x-ray beam. Since this system is not based on optical detection of the dither motion, problems associated with stray light interfering with the detection of the XEOL signal are removed. Finally, the compact and self-aligning nature of the tuning-fork technique makes it much more amenable for studies where remote operation is necessary;
(3) The XAS-SNOM head prototype performs the scan of the sample under the tip, in order to keep the tip at a fixed position with respect to the synchrotron radiation microbeam and to collect in near-field condition the x-ray excited optical luminescence emitted by the sample. Such configuration assures that the same part of the beam is always used during measurements;
(4) The XAS-SNOM instrumentation is provided with two highly sensitive detectors that the operator can alternatively connect to the same spectrograph/monochromator in order to easily carry out the topographic/optical imaging or the spectroscopic measurements.

B. The XAS-SNOM microscope prototype

As a consequence of these general choices, a custom-tailored SNOM probe head has been built, capable to operate with the commercial controller SMENA from NT-MDT. The sketch of the XAS-SNOM head prototype and of the XEOL detection/analysis setup is shown in Fig. 1.

The core of the XAS-SNOM head is the tip/sample nanopositioning system. Two towers of ultra-compact piezoelectric actuators (ANPxyz100 by Attocube) provide the microscope with a six-independent-axis system. This particular design allows the absolute alignment of the sample and of the probe with respect to each other and to the synchrotron radiation beam. After the alignment, the Attocube piezomovements do not exhibit any noise, drift, or backlash since no voltage is applied to the piezo. This grants a very high precision, stability, and reproducibility for all alignment operations.

The tip/sample nanopositioners are controlled by an inertial motor driving controller (ANC150 by Attocube), that generates the driving pulses needed by the low voltage multilayer piezostacks. In order to better adapt the capabilities of the controller to the experimental needs of the project, dedicated software has been developed, able to remotely control the ANC150. The software allows selecting the actuator tower (tip or sample), the axis of motion, the voltage, and the frequency of the movement pulses. The up-down motion for each axis can be executed in continuous or step-by-step modes.

A commercial NT-MDT piezoscanner is mounted on top of the Attocube tower that holds the sample. It is employed for the imaging and is capable of controlling three independent movements: scanning on the plane of the sample surface (X,Y) and perpendicular to it (Z axis). The probe engagement on the sample surface and the probe-sample distance

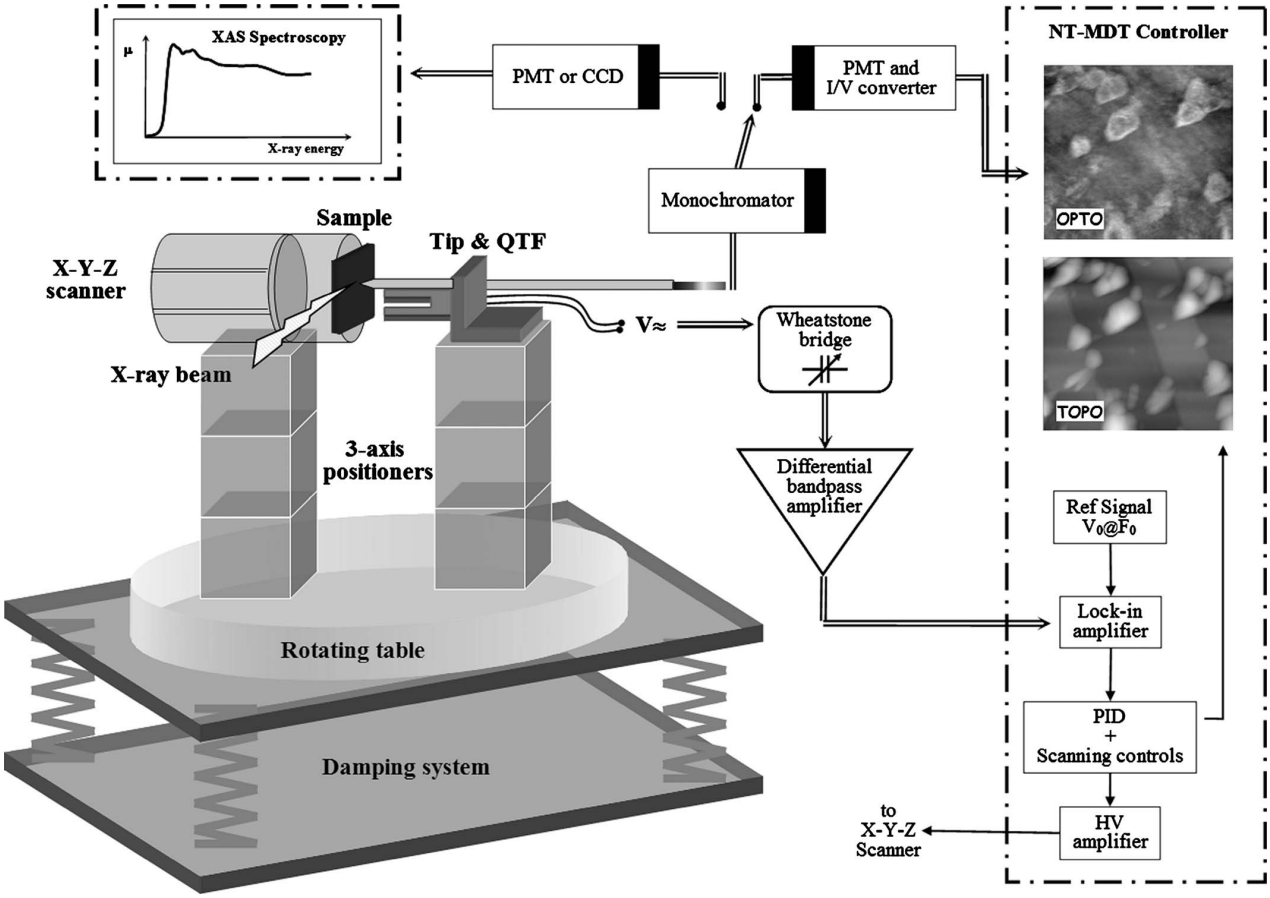

FIG. 1. Scheme of the XAS-SNOM head prototype and XEOL detection/analysis setup.

regulation during the imaging are controlled by means of the *Z* movement of the piezoscanner. The maximum scan lengths for this scanner are $18\times18\times2$ μm ($\pm10\%$). Using the maximum sampling capability of the SMENA controller (4096×4096 pixel/image), the minimum lateral scanning step is around 4 nm, and 0.4 nm for the vertical axis.

The XAS-SNOM instrumentation is completed by a sturdy circular base that gives stability to the microscope head, allowing also to change the incidence angle of the beam on the sample in the range between 0° and 40°. If necessary, a damping system positioned under the rotating table attenuates the mechanical vibrations, uncoupling the device from its support.

The microscope works in shear-force mode and the fiber tip glued on a quartz tuning fork (QTF) is used for probing the surface. A tailored electronics handles the shear-force feedback signals. The electrically excited QTF is placed in a Wheatstone bridge which eliminates the effect of its parasitic capacitance. After the amplification, the bridge signal, inherently related to the tip-sample interaction, is sent to the SMENA controller for the PID feedback. The PID loop keeps constant the tip-sample distance, when the scanner moves the sample along *XY*. The topographical image of the sample surface is obtained by monitoring the *Z* movement of the scanner. The same controller acquires the optical image, monitoring the electrical signal proportional to the intensity of the light collected by the fiber probe.

The XEOL and XEOL-XAFS spectra are recorded and displayed by another dedicated software, after undergoing a specific spectral analysis.

As concerns the acquisition setup, the main novelty introduced by the XAS-SNOM prototype stays in the near-field detection by means of a tapered optical fiber probe, directly connected to the monochromator. Other than this, the components of the detection system are the same employed in standard far-field measurements.

First, the light collected by the optical fiber enters the SpectraPro-150 spectrograph/monochromator by Acton Research Corporation. A standard mounting flange is provided to accommodate a charge coupled device (CCD) or a diode array, a second flange was designed and home fabricated to allow the mounting of the photomultiplier tube (PMT) detectors in the right focal plane.

A CCD-1100PB camera (1100×330 pixels) by Princeton Instruments is employed for fast spectral analysis of the XEOL signal. It is ideal for low light level applications requiring very long integration times in the visible spectral range.

Two different PMTs by Hamamatsu may be employed for the optical imaging, as well as for spectroscopic applica-

tions. The first one is the H5784-04 photosensor module. Due to its compactness, this PMT has been directly mounted on the XAS-SNOM head prototype to be used during the alignment procedure and for preliminary and quick test on reference samples. The second photomultiplier tube is the R928 model. This PMT features extremely high quantum efficiency, good signal-to-noise (S/N) ratio, wide spectral response and high current amplification (10^7 for a supply voltage of 1000 V dc).

Finally, in order to create a fully working prototype, the integration of the XAS-SNOM device with the beamline software control and data acquisition system has been the object of careful analysis. A protocol based on the setting and analysis of some digital lines has been developed to guarantee the synchronized and automatic management of the measurement process. This solution turned out to be the best choice, since it allows a simpler and more secure implementation of the experiment at different beamlines of a synchrotron radiation facility.

C. Optical fiber probe

As for all local probe microscopes, the heart of a SNOM lies in the quality of the tip that is raster scanned on the sample surface. In fact, the curvature radius of the probe and the size of the hole open at its very apex determine the resolution of the topographic and optical imaging, respectively. We employed two types of aperture probes.

The first one is represented by chemically etched optical fiber tips fabricated by NT-MDT. They are obtained from a single-mode optical fiber with core and cladding diameters of 3 and 95 μm, respectively. After the chemical etching, a thin aluminum coating is evaporated on the entire tip except a tiny region, whose size determines the aperture diameter (generally between 30 and 100 nm). The transmission is optimized in the 480–550 nm spectral range; the nominal optical efficiency goes from $(3-30)\times10^{-5}$ for a 100 nm aperture to $(3-30)\times10^{-6}$ for a 30 nm hole. The curvature radius and the cone angle are estimated to be 50–100 nm and $\sim20°$, respectively.

The second type of SNOM probes includes pulled optical fiber tips produced by LovaLite. They are obtained from standard single-mode Corning SMF28e fibers commonly employed in telecommunication. The apex curvature radius is about 50 nm and the tip is Al coated. The transmission coefficient of these probes is estimated by the producer in the range of $10^{-5}-10^{-4}$.

The optical fiber probes delivered by NT-MDT and LovaLite came just tapered and metalized. Using a purpose-built instrumentation, the tips were glued to one prong of the quartz tuning fork mounted on the specific epoxy holder. This is the most delicate phase in the assembling of the tuning fork and probe holder. The tip has to be glued perfectly parallel to the prong arm, protruding less than 1 mm out of the prong and using the smallest amount of glue. These expedients help to leave essentially unchanged the resonant frequency of the overall system. Finally, the optical fibers were terminated with FC-type connectors.

D. Prototype characterization in the laboratory

An in house characterization of the XAS-SNOM prototype has been carried out before installing the microscope head at a synchrotron radiation facility. The experiment, performed at the CRMC-N laboratory of Marseille (France), consisted in the simultaneous acquisition of the topographic and optical images by detecting the sample optical luminescence emission excited by means of an external light source.

The XAS-SNOM head has been mounted on top of an optical bench; the exciting source, a 325 nm wavelength He–Cd laser (5 mW), has been focused on the sample surface: a silica grating with stoichiometric ZnO nanoparticles randomly dispersed on it. ZnO is a wide band-gap material that, under proper excitation, exhibits a defect-related optical luminescence in the visible range and an excitonic band in the ultraviolet region. The optical fiber tip collects the near-field photons emitted by the surface and guides them directly to the PMT-H5784. To prevent the scattered laser light from entering the PMT detector, a notch filter has been placed at the end of the optical fiber.

These images provide valuable information on the imaging capabilities of the XAS-SNOM instrumentation. As shown in Fig. 2, in a conventional laboratory environment the microscope prototype produces highly resolved topographic and optical images with a lateral resolution down to 100–200 nm. The topographic vertical resolution is about 2–3 nm and is limited by the noise of the piezoscanner signal in the Z direction.

The imaging quality is strongly dependent on the optical fiber probe, namely, on its size and shape when detecting the shear-force signal and on the small aperture features when the optical signal is collected through the tip hole.

III. APPLICATIONS TO SYNCHROTRON RADIATION

A. Near-field XAS-XEOL spectroscopy

The XAS-SNOM prototype has been employed to perform local x-ray absorption measurements in near-field XEOL detection mode at the European Synchrotron Radiation Facility in Grenoble (France). Two different beamlines were used: the first experiments were performed at the BM05 beamline, located at a bending magnet source and equipped with a double-crystal Si(111) monochromator; later, we had access to the ID03 beamline, which has been very recently renovated and allows to use different undulators in series to reach a very intense, collimated beam before a channel-cut Si(111) monochromator. Two different Kirkpatrick-Baez (KB) optics, especially optimized for BM05 and ID03 beamlines, were used for microfocusing the x-ray beam: the size of the microbeam at the sample was 2×3 μm^2 (at BM05) and 5×5 μm^2 (at ID03), being much larger than the hole size of the tip, and not varying too much with time.[25] For this reason, at least at the present state of art, we may consider the photon distribution in the microbeam as homogeneous. The main difference between the two beamlines was the photon intensity on the sample, and the energy range tunability (determined by the KB optics). The x-ray absorption near-edge structure (XANES)-XEOL signal was calculated as the ratio of the XEOL signal intensity (I) and the incoming beam

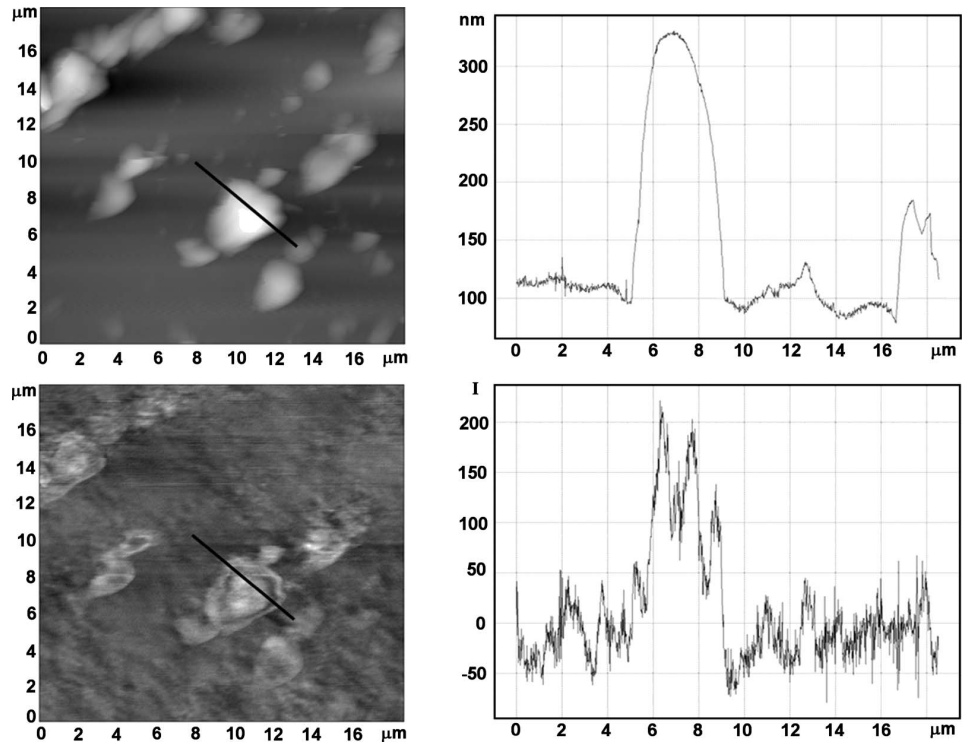

FIG. 2. Couples of topographic (top) and optical (bottom) images (18×18 μm^2) of a silica grating with stoichiometric ZnO particles randomly dispersed on it. The arbitrary section profiles along the indicated lines are also reported.

intensity (I_0). The latter was measured using the incoming beam monitor (diode), located at the exit of the KB focusing device. In this way, the XANES measurements are independent on the normal intensity decay with time of the synchrotron beam.

In this experiment, the optical fiber tip was used at first to image the sample surface topography; after that, the probe was placed in various points of interest and kept at the same position in near-field condition while the x-ray energy was tuned across the K or L_3 absorption edge of a specific chemical element. The XANES spectrum was obtained plotting the XEOL intensity at a selected wavelength (or range of wavelengths) as a function of the x-ray energy.

Figure 3 presents the interesting results obtained for a ZnO nanostructured thin film deposited by dc magnetron sputtering on a Si substrate and annealed in air at about 800 °C for 8 hours. The upper line shows the XANES-XEOL spectrum at the Zn K-edge acquired in far-field conditions, using a lens for collecting the light.[26] As expected, the x-ray absorption fine structures exhibited by this film well reproduce the oscillation features typical of a ZnO polycrystalline powder (not shown). The middle and bottom lines of Fig. 3 present the same XANES-XEOL spectra recorded in near-field condition at ESRF-BM05 and ESRF-ID03 beamlines using the XAS-SNOM head microscope. In this case, the optical fiber tip is probing the x-ray excited optical luminescence (around the band maximum wavelength at 540 nm) emitted by a region of the sample surface as small as the tip aperture, that is nominally about 100 nm. The SNOM probe is capable of collecting the weak XEOL signal in the operational conditions imposed by the experiment and by the synchrotron environment. To our knowledge, this is the first time that near-field XANES-XEOL spectra are recorded by means of a custom-tailored SNOM microscope integrated on a synchrotron radiation facility. Despite of the noisy signal, the near-field x-ray absorption features reproduce the exact fingerprint of the ZnO nanostructured material deposited on the Si substrate. The reproducibility of all acquired spectra has been checked out, obtaining positive and promising results in terms of system and x-ray beam stability. A much higher signal-to-noise ratio has been observed when the more intense synchrotron radiation beam has been used, namely, passing from an exciting source of 10^{13} photon/s mm^2 (ESRF-BM05) to one of about 10^{15} photon/s mm^2 (ESRF-ID03). As a direct consequence of the XEOL signal enhancement, the XANES-XEOL spectra exhibit more defined and better resolved modulations of the absorption coefficient.

Unfortunately, at high x-ray photon density, the contribution to the XEOL signal coming from defects activated by x-rays in the optical fiber tip becomes important. For this reason, great attention has to be paid to the position of the probe with respect to the synchrotron radiation beam. The very apex of the tip has to be as retracted as possible from the beam, while the x-ray beam has to impinge onto the sample region just under the tip.

B. Topography and XEOL-optical imaging

The second kind of experiments carried out at ESRF-ID03 is the element-specific profilometry, consisting in a

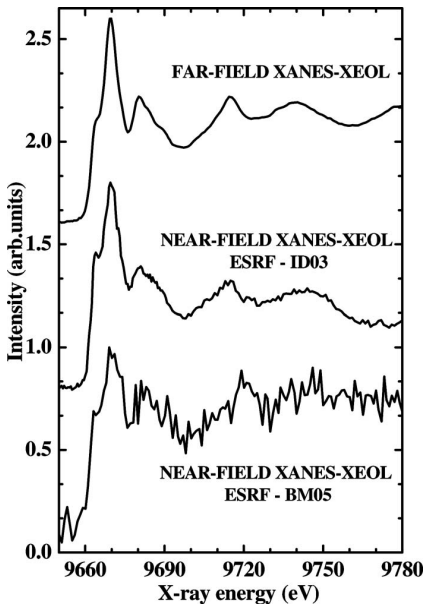

FIG. 3. Comparison of Zn *K*-edge XANES-XEOL spectra of a nanostructured ZnO thin film acquired at ESRF in different configurations: standard far-field (top), through the SNOM probe in near-field conditions at the undulator beamline ID03 (middle) and at the bending-magnet beamline BM05 (bottom).

conventional scanning microscopy technique enriched by sensitivity to chemical elements distribution. This is achieved by setting the x-ray energy below or above the absorption edge of a specific element and by detecting, for each energy, the x-ray excited optical luminescence in the near-field condition while scanning the sample surface with the probe. The optical contrast is obtained by calculating the difference between two images above and below the absorption edge: it provides a map of the luminescent centers containing the selected chemical element with the spatial resolution offered by the subwavelength aperture of the optical fiber probe.

As an example of this application, we report in Fig. 4 some images (topographic and optical) obtained at ID03-ESRF for a dc magnetron sputtered mixed $ZnWO_4$–ZnO thin film. The images have been recorded below and above the W L_3 edge. Note that the x-ray energy above the edge has been chosen to correspond to the position of the white line maximum, to maximize the change in the XEOL intensity. The slow monotonic decrease of the x-ray beam intensity during two consecutive measurements was monitored and found negligible in respect to the changes of the XEOL intensity due to the nanostructures present in the sample.

The topographic images reported in Fig. 4 document that we were able to achieve at ESRF a good spatial resolution, comparable with that provided by the same instrument in a standard laboratory environment. The reproducibility of the topographic images is quite satisfactory. To reach this goal at ID03, we had to develop a specific damping stage, capable of attenuating the mechanical vibrations transmitted to the prototype by the noisy environment of the synchrotron radiation beamline.

From the characterization by x-ray diffraction, micro-

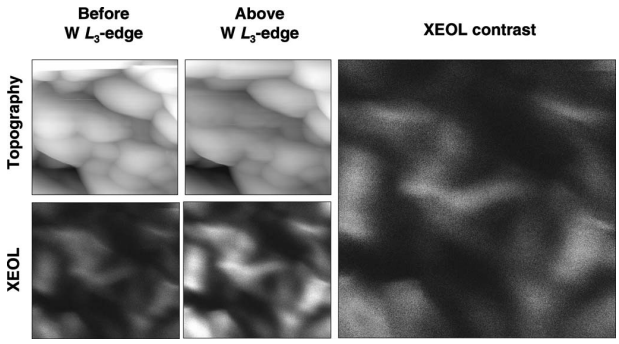

FIG. 4. Topography (small, top) and XEOL (small, bottom) images of a $ZnWO_4$–ZnO thin film obtained simultaneously at two different x-ray energies. The XEOL contrast image (large, on the right) corresponds to the difference between the two XEOL images measured above and below the W L_3 edge and detected at about 500 nm. The images size is 18×18 μm^2.

Raman, and AFM, we know that this film is composed of nanocrystalline $ZnWO_4$ and ZnO,[27] finely mixed within the grains visible in the topographic image. The luminescence of the mixed $ZnWO_4$–ZnO thin film originates both from the oxyanionic WO_6 groups in zinc tungstate[28] and from excitonic and defect recombination bands in zinc oxide.[29] Only the excitonic band of ZnO, if detectable, is well separated from the zinc tungstate contribution. On the contrary, the photoluminescence bands in the visible of both components are almost superimposed.[28–30] The two XEOL images presented in Fig. 4 have been recorded by tuning the optical monochromator at about 500 nm, in the range of the maximum XEOL intensity: they have been measured consecutively, simultaneously with the topographic images, by setting the x-ray excitation energy below and above the W L_3 edge. The XEOL contrast image has been calculated as the difference (pixel by pixel in a 256 points gray scale) between two XEOL images. Thus, the bright features on the XEOL contrast image (bigger image on the right side of Fig. 4) correspond to the distribution of those luminescent centers that are directly related to the x-ray absorption by W atoms. We may note that $ZnWO_4$ is not segregated in particular grains of the sample.

The microscope has been proved capable of high imaging reproducibility, confirming that the observed features are actually related to the topographical and near-field optical properties of the sample. By repeating this kind of measurements, the XAS-SNOM detection setup has shown a good sensitivity to small variations of the optical signal, both by scanning the x-ray energy across different absorption edges and by probing surfaces characterized by different chemical, morphological and optical properties. A similar, but not identical, XEOL contrast image has been recorded also at the Zn *K* edge.[27] In order to detect only the luminescence coming from ZnO or $ZnWO_4$, the same XEOL images have to be repeated at different wavelengths. This will be the goal of future studies, together with an effort to better define the range of application of this prototype to diluted systems.

Further measurements are in progress to characterize the lateral resolution of the SNOM image, in comparison with the topographic one: in fact, the latter is determined by the

shape and dimension of the tip, while the optical image should have a much better resolution because of the reduced dimensions of the hole in the metallic coating.

IV. CONCLUSIONS

In this paper we have presented a novel instrumentation that combines synchrotron radiation and SNOM local probe detection in a unique characterization tool.

The XAS-SNOM microscope prototype collects the XEOL in near field using a tapered optical fiber probe, glued to an oscillating quartz tuning fork. A shear-force feedback is employed both to regulate the probe-sample distance and to record the topographical image of the surface. The absolute positioning of the tip and of the sample with respect to the x-ray microbeam is performed using a six-independent-axis system. In order to collect the XEOL signal by means of the optical fiber tip, the imaging is carried out scanning the sample under the probe, that is kept fixed with respect to the radiation beam.

The XAS-SNOM microscope device has been specifically manufactured to operate in conjunction with x-ray microbeams in the harsh synchrotron radiation environment. It has been successfully installed at the European Synchrotron Radiation Facility and integrated with the beamline software control and data acquisition system. With the employment of a custom-tailored antivibration system, this setup commonly achieves a lateral resolution of about 100–200 nm, while in the vertical direction the resolution is about 3 nm.

First tests of the new XAS-SNOM microscope head have been done on pure ZnO and mixed $ZnWO_4$–ZnO nanostructured thin films, due to the intense optical luminescence of these samples under x-ray excitation and to their interest for a wide range of technological and scientific applications.[31] Thanks to the coupling of x-ray absorption and near-field optical detection, we have successfully performed experiments of element-specific profilometry, in which conventional SNOM microscopy is enriched by sensitivity to chemical elements. By comparing different optical images, it is already possible to obtain atomic maps of both Zn and W distributions; moreover, we are currently testing a methodology to obtain also maps of ZnO and $ZnWO_4$ distribution.[30]

We have also recorded high quality XANES spectra, using synchrotron radiation as exciting source and collecting the XEOL signal in near-field condition. This allows studying the local atomic structure and electron density of states only of those absorbing atoms that are near the optical emission centers in the small region probed by the tip.

The results achieved so far in thin films samples are quite promising in order to reach the more ambitious goals to measure XEOL of diluted luminescent nanostructures or of isolated nanodots with quantum confinement properties. This will be the object of future studies. The application of the XEOL spectroscopy to samples containing nanodots and nanowires using far-field detection is currently performed in various Synchrotron Radiation Facilities,[17,32–35] but with no possibility to study single nanostructures, nor to know the morphology of the investigated region. The new XAS-SNOM microscope we have developed allows the alignment of a selected region of a luminescent sample in respect with micro focused x-ray beams and the detection of XEOL spectra with the spatial resolution of the SNOM tip. The acquisition of good XAS spectra is strongly dependent, however, from the XEOL intensity and from its relative change when crossing an absorption edge. In any case, future studies of isolated nanostructures will require the use of very intense and stable x-ray microbeams. Great improvements of the new XAS-SNOM technique can be performed by increasing the stability of the experimental setup, with a dedicated end station. One of the main problem is coming from the de-coupling of the x-ray focusing device and the microscope (containing SNOM head and sample nanopositioners). A further subject of improvement is the selection and production of more reliable SNOM tips, having less problems of radiation damage and, possibly, a higher optical resolution and transmission.

This research project holds out promise for future developments not only of the combined XAS-SNOM technique but, more in general, of the joint use of scanning probe microscopies and x-ray absorption techniques. In confirmation of this, more and more works and scientific publications are available in literature that point out the possible benefits of using, for example, a metallic tip to collect the photoemitted electrons in tunneling conditions[36,37] or to measure the local charge density.[38,39]

The search for innovative tools capable of investigating and characterizing the new phenomena associated with confined systems is still at the dawn. The feasibility study performed so far has demonstrated that an approach based on local tip detection of x-ray absorption yields can provide an invaluable tool to obtain fundamental information on structural, electronic, and optical properties of matter at the nanoscale.

ACKNOWLEDGMENTS

This work has been supported by the European Commission under the 6th Framework Programme (Specific Targeted Research Project No. STRP 505634-1: X-TIP). We acknowledge the cooperation and active discussion of the partners of the project, in particular, G. Dalba, O. Dhez, R. Felici, and F. Comin. The XEOL measurements have been performed at the European Synchrotron Radiation Facility (ESRF-Grenoble, France), using public and industrial beam time. We thank the cooperation of the staff of BM05 and ID03 beamlines of ESRF for their valuable participation to the experiments. In house characterization of the XAS-SNOM prototype has been carried out at the CRMC-N laboratory of Marseille (France). We thank W. Marine, Y. Mathey, and D. Tonneau for their cooperation and active participation. R. Kalendarev (ISSP, University of Latvia, Riga) is acknowledged for the preparation of mixed $ZnWO_4$–ZnO nanostructured thin films.

[1] K. Lahtonen, M. Lampimäki, P. Jussila, M. Hirsimäki, and M. Valdena, Rev. Sci. Instrum. **77**, 083901 (2006).
[2] M. Staderman, H. Grube, J. J. Boland, S. J. Papadakis, M. R. Falvo, R. Superfine, and S. Washburn, Rev. Sci. Instrum. **74**, 3653 (2003).

[3] C. E. Jordan, S. J. Stranick, R. R. Cavanagh, L. J. Richter, and D. B. Chase, Surf. Sci. **433**, 48 (1999).
[4] D. Zeisel, V. Deckert, R. Zenobi, and T. Vo-Dinh, Chem. Phys. Lett. **283**, 381 (1998).
[5] S. Webster, D. A. Smith, D. N. Batchelder, and S. Karlin, Synth. Met. **102**, 1425 (1999).
[6] U. Durig, D. W. Pohl, and F. Rohner, J. Appl. Phys. **59**, 3318 (1986).
[7] G. A. Massey, J. A. Davis, S. M. Katnik, and E. Omon, Appl. Opt. **24**, 1498 (1985).
[8] A. Piednoir and F. Creuzet, Micron **27**, 335 (1996).
[9] M. K. Hong, A. G. Jeung, N. V. Dokholyan, T. I. Smith, H. A. Schwttman, P. Huie, and S. Erramilli, Nucl. Instrum. Methods Phys. Res. B **144**, 246 (1998).
[10] C. A. Michaels, S. J. Stranick, L. J. Richter, and R. R. Cavanagh, J. Appl. Phys. **88**, 4832 (2000).
[11] D. Vobornik, G. Margaritondo, J. S. Sanghera, P. Thielen, I. D. Aggarwal, B. Ivanov, N. H. Tolk, V. Manni, S. Grimaldi, A. Lisi, S. Rieti, D. W. Piston, R. Generosi, M. Luce, P. Perfetti, and A. Cricenti, J. Alloys Compd. **401**, 80 (2005).
[12] A. Cricenti, R. Generosi, M. Luce, P. Perfetti, G. Margaritondo, D. Talley, J. S. Sanghera, I. D. Aggarwal, N. H. Tolk, A. Congiu-Castellano, M. A. Rizzo, and D. W. Piston, Biophys. J. **85**, 2705 (2003).
[13] D. Vobornik, G. Margaritondo, J. S. Sanghera, P. Thielen, I. D. Aggarwal, B. Ivanov, J. K. Miller, R. Haglund, N. H. Tolk, A. Congiu-Castellano, M. A. Rizzo, D. W. Piston, F. Somma, G. Baldacchini, F. Bonfigli, T. Marolo, F. Flora, R. M. Montereali, A. Faenov, T. Pikuz, G. Longo, V. Mussi, R. Generosi, M. Luce, P. Perfetti, and A. Cricenti, Infrared Phys. Technol. **45**, 409 (2004).
[14] B. Knoll and F. Keilmann, Nature (London) **399**, 134 (1999).
[15] A. Larhech, R. Bachelot, P. Gleyzes, and A. C. Boccara, Appl. Phys. Lett. **71**, 575 (1998).
[16] G. Martínez-Criado, A. Somogyi, A. Homs, R. Tucoulou, and J. Susini, Appl. Phys. Lett. **87**, 061913 (2005).
[17] G. Martínez -Criado, B. Alen, A. Homs, A. Somogyi, C. Miskys, J. Susini, R. Tucoulou, J. Pereira, and J. Martinez-Pastor, Appl. Phys. Lett. **89**, 221913 (2006).
[18] N. R. J. Poolton, B. Hamilton, and D. A. Evans, J. Phys. D **38**, 1478 (2005).
[19] N. R. J. Poolton, B. M. Towlson, B. Hamilton, and D. A. Evans, Nucl. Instrum. Methods Phys. Res. B **246**, 445 (2006).
[20] H. C. Kang, J. Maser, G. B. Stephenson, C. Liu, R. Conley, A. T. Macrander, and S. Vogt, Phys. Rev. Lett. **96**, 127401 (2006).
[21] G. G. Schroer, O. Kurapova, J. Patommel, P. Boye, J. Feldkamp, B. Lengeler, M. Burghammer, C. Riekel, L. Vincze, A. van der Hart, and M. Kuchler, Appl. Phys. Lett. **87**, 124103 (2005).
[22] D. H. Bilderback, S. A. Hoffman, and D. J. Thiel, Science **263**, 201 (1994).
[23] A. Snigirev, A. Bjeoumikhov, A. Erko, I. Snigireva, M. Grigoriev, M. Erko, and S. Bjeoumikhova, J. Synchrotron Radiat. **14**, 227 (2007).
[24] K. Karrai and R. Grober, Appl. Phys. Lett. **66**, 1842 (1995).
[25] E. Ziegler, S. de Panfilis, L. Peverini, P. van Vaerenbergh, and F. Rocca, AIP Conf. Proc. **879**, 1349 (2007).
[26] S. Larcheri, C. Armellini, F. Rocca, A. Kuzmin, R. Kalendarev, G. Dalba, R. Graziola, J. Purans, D. Pailharey, and F. Jandard, Superlattices Microstruct. **39**, 267 (2006).
[27] S. Larcheri, F. Rocca, D. Pailharey, F. Jandard, R. Graziola, A. Kuzmin, R. Kalendarev, and J. Purans, "A new tool for nanoscale X-ray absorption spectroscopy and element specific SNOM microscopy," Micron (2008).
[28] T. Oi, K. Takagi, and T. Fukazawa, Appl. Phys. Lett. **36**, 278 (1980).
[29] S. J. Pearton, D. P. Norton, K. Ip, Y. W. Heo, and T. Steiner, Prog. Mater. Sci. **50**, 293 (2005).
[30] S. Larcheri, F. Rocca, D. Pailharey, F. Jandard, R. Graziola, G. Dalba, A. Kuzmin, R. Kalendarev, and J. Purans, "Nanostructure of mixed $ZnWO_4$ thin film probed by combined XAS-SNOM technique," (to be publish).
[31] Z. L. Wang, J. Phys.: Condens. Matter **16**, R829 (2004).
[32] G. Dalba, N. Daldosso, P. Fornasini, M. Grimaldi, R. Grisenti, and F. Rocca, Phys. Rev. B **62**, 9911 (2000).
[33] G. Dalba, N. Daldosso, P. Fornasini, R. Grisenti, L. Pavesi, F. Rocca, G. Franzó, F. Priolo, and F. Iacona, Appl. Phys. Lett. **82**, 889 (2003).
[34] T. K. Sham, S. J. Naftel, P.-S. G. Kim, R. Sammynaiken, Y. H. Tang, I. Coulthard, A. Moewes, J. W. Freeland, Y.-F. Hu, and S. T. Lee, Phys. Rev. B **70**, 045313 (2004).
[35] Y. L. Soo, S. W. Huang, Y. H. Kao, V. Chhabra, B. Kulkarni, J. V. D. Veliadis, and R. N. Bhargava, Appl. Phys. Lett. **75**, 2464 (1999).
[36] K. Tsuji, K. Wagatsuma, K. Sugiyama, K. Hiraga, and Y. Waseda, Surf. Interface Anal. **27**, 132 (1999).
[37] A. Saito, J. Maruyama, K. Manabe, K. Kitamoto, K. Takahashi, K. Takami, M. Yabashi, Y. Tanaka, D. Miwa, M. Ishii, Y. Takagi, M. Akai-Kasaya, S. Shin, T. Ishikawa, Y. Kuwahara, and M. Aono, J. Synchrotron Radiat. **13**, 216 (2006).
[38] S. M. Gray, J. Electron Spectrosc. Relat. Phenom. **109**, 183 (2000).
[39] M. Ishii, B. Hamilton, N. R. J. Poolton, N. Rigopoulos, S. De Gendt, and K. Sakurai, Appl. Phys. Lett. **90**, 063101 (2007).